Earthquake Geotechnical Engineering for Protection and Development of Environment and Constructions – Silvestri & Moraci (Eds)
© 2019 Associazione Geotecnica Italiana, Rome, Italy, ISBN 978-0-367-14328-2

Modelling the dynamic response of gravity retaining wall systems using OpenSees

A. Kamalzadeh & M.J. Pender
The University of Auckland, Auckland, New Zealand

ABSTRACT: Recent work using the OpenSees finite element software to model the response of gravity retaining walls to Ricker wavelets is presented. The behaviour of the wall system during earthquake loading is controlled by the capacity of the shallow foundation supporting the wall. OpenSees is used to verify our contention that the primary mode of failure is one of rotational deformation rather than horizontal sliding. For situations where a gravity wall is founded on a rock layer or very hard soil, the horizontal acceleration at limiting equilibrium of the wall is controlled by sliding of the wall system on the foundation layer. For all other cases, a rotational failure mechanism based on mobilising the moment capacity of the foundation controls the limiting horizontal acceleration. Simple modelling shows that the horizontal acceleration to initiate rotational failure of the foundation is less than that to initiate sliding failure. Consequently, the design criteria for gravity walls is the residual displacement generated by rotation at foundation level during the course of the earthquake. Using the realistic cyclic stress-strain models available in OpenSees we have appropriate representations of the cyclic nonlinear behaviour of the cohesionless soil backfill and cohesionless soil beneath the foundation of the wall. The finite element modelling illuminates the understanding we have obtained from simple design analyses and enables us to evaluate the accumulation of permanent displacement during the course of the input excitation.

1 INTRODUCTION

The current design approach can be traced back to 1g shaking table tests observations performed by Okabe (1924) and Mononobe & Matsuo (1929), the so-called M-O approach. With some modifications by Seed and Whitman (1970) the M-O method has become the main approach for designing earthquake-resistant retaining structures. The appeal of this method is its simple application. Formula 1 to 3 show how the M-O lateral thrust is calculated.

$$K_{AE} = \frac{\cos^2(\varphi - \theta - \alpha)}{\cos\theta\cos^2\alpha\cos(\alpha + \delta + \theta)\left(1 + \sqrt{\frac{\sin(\varphi+\delta)\sin(\varphi-\theta-i)}{\cos(\alpha+\delta+\theta)\cos(i-\alpha)}}\right)^2} \tag{1}$$

$$\theta = tan^{-1}\left(\frac{k_h}{1 - k_v}\right) \tag{2}$$

$$P_{AE} = 0.5K_{AE}\gamma H^2 \; with P_{AEh} = P_{AE}cos\delta \; and P_{AEv} = P_{AE}sin\delta \tag{3}$$

Where φ is the backfill friction angle, α is the angle between the backfill side of the wall with the vertical, δ is the interface friction angle, i is the backfill surface slope angle, γ is the unit weight of the backfill and, H is the height of the wall. Note that in the absence of a dynamic excitation ($\theta = 0$) therefore, we can calculate pressures induced by soil self weight. Note that in this study the vertical acceleration is assumed to be zero ($k_v = 0$).

Although, recent design approaches concludes the equivalent static seismic force distribution along the depth of the wall is similar to an inverted triangle, using centrifuge test and FE

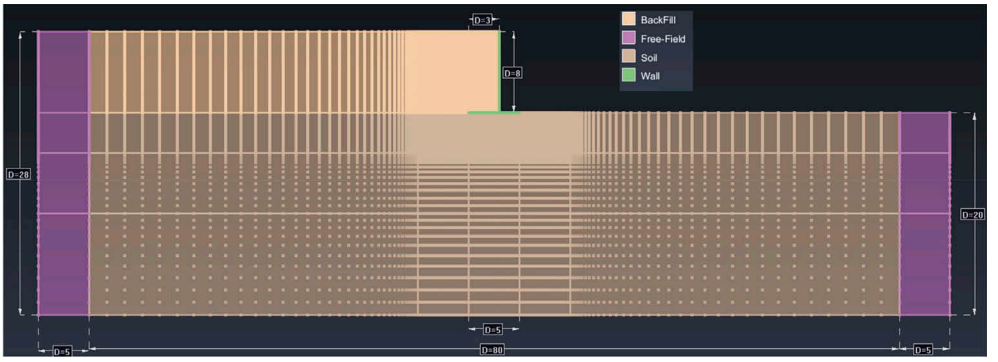

Figure 1. Geometry of the model

modelssome researchers currently found out it is an upright triangle (Mikola et al., 2014, Chin et al., 2016, Wood, 2018). Moreover, another source of overestimation is the estimation of the equivalent force magnitude, especially where design PGA (peak ground acceleration) exceeds 0.4g (Sitar et al., 2012). The current design method assumes maximum dynamic earth pressure is simultaneous with the wall peak inertia force causing over-conservative design while centrifuge test results have shown the occurrence time of these is not coincident (Sitar and Al Atik, 2008). Al Atik and Sitar (2010) have implemented finite element (FEM) analyses using the OpenSees (McKenna et al., 2013) platform (developed by The University of Berkley, California) to model their centrifuge tests and full-scale models. They find the FEM analyses results from OpenSees are in strong agreement with centrifuge test results and find the current design method is excessively conservative. Also, Chin et al. (2016) used OpenSees modelling and localised their models using typical New Zealand soil types and seismic zones of NZS 1170.5 (Standards New Zealand Technical Committee, 2004) for embedded cantilever walls with two different propping configurations.

In this study, we used OpenSees to model soil-retaining wall problem types. The GiD (Coll et al., 2016) pre-processing software, has been utilised to build the geometry of the model.The soil profile is assumed to have unlimited lateral extent, and there is a bedrock lying under the model. The wall dimensions are the same as one of the cases in Pender (2018) paper. The static and dynamic response of the wall is investigated.

2 SOIL-STRUCTURE MODEL

2.1 *Model construction*

The 2D soil – gravity cantilever retaining wall is modelled in the OpenSees (McKenna et al., 2013). The soil profile is assumed unlimited in the horizontal direction hence, only a small portion of it around the retaining wall is modelled which we call it the interior model. To establish an accurate model, the interior model has a mesh size of 10cm in the proximity of the retaining wall. However, the mesh becomes larger as we move on to the sides of the model.

All the soil elements are of a four-noded, quadrilateral, plane-strain type with a single robust integration point (Gauss point) and, two translational degrees of freedom (DOF) at each node. These elements are called SSPquad in the OpenSees. The interior model has a length of 80m, depth of 20m and 8m backfill on the left side, see Figure 1. Assuming the soil profile has large lateral extent, two blocks of soil columns have been modelled at both sides of the interior model. The out of plane thickness of these columns are significant, 10,000m, to represent the mass of the assumed infinite soil profile. Periodic boundary condition is simulated to ensure the vertical shear wave propagation in these soil columns. This means in a single soil column, the nodes at the same level, are tied together in both directions using the equalDOF command in the OpenSees as in Figure 2 (McGann and Arduino, 2015). The free-

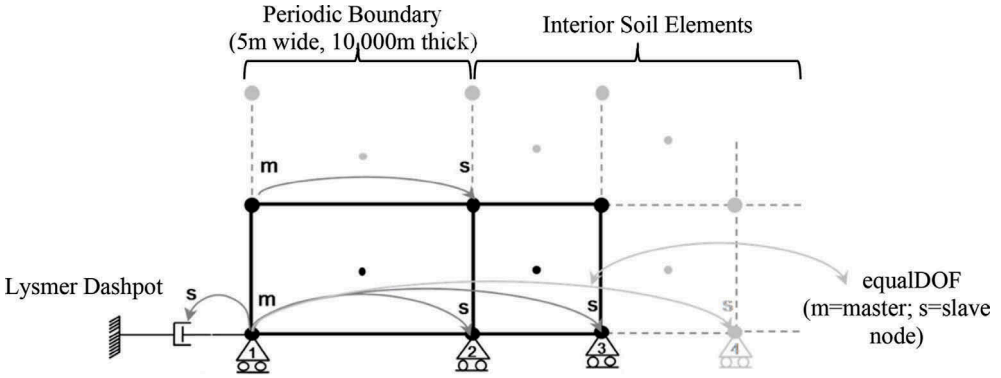

Figure 2. Dynamic analysis boundary conditions at bottom left corner (After Chin et al. (2016))

field columns are approximately situated at 40m distance from the wall to eliminate any influence that this boundary may have on the retaining wall area.

During the static analysis, the base of the model is fixed in both directions while throughout the dynamic analysis the vertical DOF is fixed. All the nodes at the base (slave) are tied to the bottom left corner node (master) horizontally. To avoid trapping the shear waves in the system, a zero-length dashpot with a viscous material at the bottom left corner, known as Lysmer-Kuhlemeyer dashpot (1969), is used to play the role of the elastic half-space beneath the model. While one end of the dashpot in fixed in both directions, the other end is tied horizontally to the master soil node at the bottom left corner. Employing Joyner and Chen (1975) approach, the viscous material damping coefficient is the product of mass density and shear wave velocity of the presumed elastic half-space underneath the model. This elastic half-space is a bedrock with a density of 2.4 t/m^3 and shear wave velocity of 1800 m/s.

The gravity cantilever retaining wall is simulated using two-node elastic beam-column elements with two translational DOFs and a rotational one at each node. This wall is considered to be reinforced concrete with an elastic modulus of 30 GPa and a density of 2.3 t/m^3. The weight of the wall is applied at each node. The dimensions of the wall are similar to one of the Pender (2018) examples: 8m in height, 5m long foundation, 3m heel length, and all components 0.5m thickness.

The interfaces between the wall and soil nodes have two main characteristics. They can only behave in compression in their local axial axis, i.e. they should detach in case of tension and, their local lateral behaviour should be frictional. For this purpose, Flat Slider Bearing elements incorporated with simple Coulomb friction model has been utilized. The chosen stiffness of the element in the frictional direction is 3900 KPa (Drumm and Desai, 1986) and the axial stiffness is the outcome of trial and error based on the recommendations of Chin et al. (2016) and Kolay et al. (2013). The interface friction angle is equal to the underlying soil friction angle ($\delta/\varphi_{Soil} = 1.0$) under the foundation. In addition, to prevent any impact effect during the dynamic analysis caused by partial uplift of the foundation or detachment of wall stem, a damping of five percent is incorporated in the axial behavior of the interfaces. It should be noted that the Rayleigh damping of the main system, does not have any effect on the interfaces.

2.2 *Constitutive soil model*

OpenSees database offers a variety of constitutive models to represent the soil. Our objective is to model dry cohesionless soil. Therefore, Manzari and Dafalias constitutive model (Dafalias and Manzari, 2004) employed. Manzari and Dafalias soil model is capable of modelling the cohesionless soil plasticity, cycling and dilative behaviour. The appeal of using Manzari and Dafalias over other constitutive models is its ability to show the peak shear strengths (not to confuse with the ultimate/critical shear strength at high strains) of dry sands at low confining pressures. This can be interesting as the mean stress in the backfill and the underlying soils

in our problem type would probably be of low values. The reason is the only vertical load in the system comes from the soil and wall self-weights.

The soil properties used in this study are derived from Dafalias and Manzari (2004) for Toyoura sand. The denseness of the soil in the Manzari and Dafalias constitutive model can be defined by the initial void ratio (e_o), the higher e_o, the softer the soil. See Table 1 for the main soil properties. As can be seen, the underlying soil is dense and, the backfill is relatively looser.

2.3 *Input excitation*

A Ricker wavelet (Fardis et al., 2003), has been used as the acceleration excitation input. The attraction of utilising this particular wavelet is the pulse-like shape of the wave and, the simplicity of interpreting the model response comparing to an earthquake record. The equation of this artificial wavelet is given by:

$$f(b,t) = \left[6b - 24b^2(t-t_o)^2 + 8b^3(t-t_o)^4\right] e^{-b(t-t_o)^2} \tag{4}$$

$$b = (\pi f)^2 \tag{5}$$

Where t is time, t_o is the time at which the Ricker wavelet magnitude is maximum, and f is the frequency. The magnitude of the Ricker wavelet is then modified to reach a desired value of acceleration. For determination of a proper value for the frequency of the Ricker wavelet a series of site response analyses have been done on a 1D soil column with a depth of 20m using OpenSees. The underlying bedrock is simulated using the approach discussed in section 2.1. The soil material is the same as the underlying soil in Table 1. A total number of 33 analyses are done for frequencies of 0.1, 0.25, 0.5, 0.75, 1.0, 1.25, 1.5, 2.0, 3.0, 4.5 and, 6.0 Hz for each 0.2g, 0.5g and, 1.0g accelerations. The results are the normalised acceleration response spectrum at the surface of the 1D soil column shown in Figure 3a.

Table 1. Soil layers main properties

	Unit	Underlying Soil	Backfill Soil	Bedrock
Depth	m	20.0	8.0	∞
Density (ρ)	t/m^3	2.0	1.9	2.4
Shear Wave Velocity (Vs)	m/s	148	132	1800
Initial Void Ratio (e_o)	-	0.6	0.8	-
Initial Shear Modulus (G_o)	MPa	43.9	32.7	-
Friction Angle (φ)	degrees	42	33	-
Static Poisson's Ratio (ν_{st})	-	0.30	0.30	-
Dynamic Poisson's Ratio (ν_{dyn})	-	0.05	0.05	-

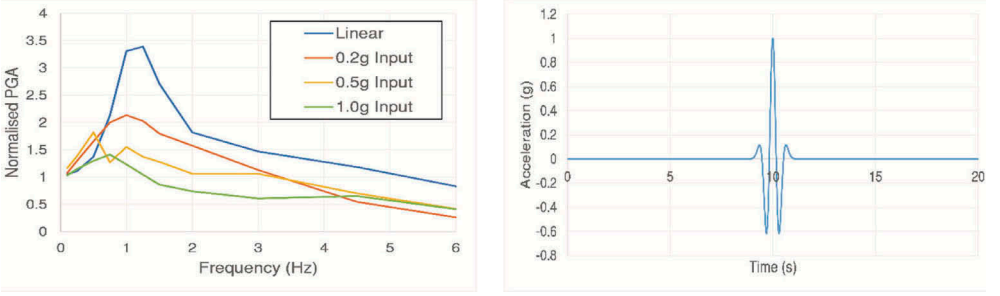

Figure 3. a) Acceleration site response of the 1D soil column and, b) 1.0g Ricker wavelet with f=1.0Hz

Figure 3a is showing for the investigated 1D soil column; the normalised peak ground acceleration is almost at its highest point in the vicinity of f=1.0Hz. Therefore, this frequency is chosen for the soil-retaining wall model input excitation.

3 ANALYSIS

This study has the advantage of using parallel processing version of OpenSees incorporated in New Zealand e-Science Infrastructure high performance computers (NeSI HPC) to analyze the models. A Rayleigh damping of two percent is considered for the model (note that this does not affect the interfaces, see section 2.1). Out of available algorithm options in the OpenSees, by conducting trial and error, Krylov Newton has been employed as it led to more robust and stable results. SeismoSignal (Antoniou et al., 2008), a signal processing software, is deployed to convert acceleration wavelets to velocity time histories and then feed them as load time histories to the left bottom corner of the model as discusses in section 2.1.

3.1 *Static phase*

Throughout the static phase, the model is only analyzed for the soil and the gravity cantilever retaining wall weights to simulate in-situ stress state. As can be seen in Figure 4a the foundation corner at the backfill side settled more than the other corner. This implies although one would expect that the retaining wall to rotate away from the backfill, our retaining wall has tilted towards the backfill. However, as the lateral displacement of the wall stem in Figure 4b illustrates, the backfill soil pushes the wall outwards. The base of the wall has been constrained to the foundation hence, the curve in the lateral displacement of Figure 4b. Figure 4c compares the static earth pressure distributions on the wall.

The equivalent earth thrust for the OpenSees and M-O earth pressures are 186 and, 177 KN respectively while their point of application is 2.78 and (8/3)=2.67m. Therefore, the magnitude of the equivalent active force and its point of application is almost the same in both approaches.

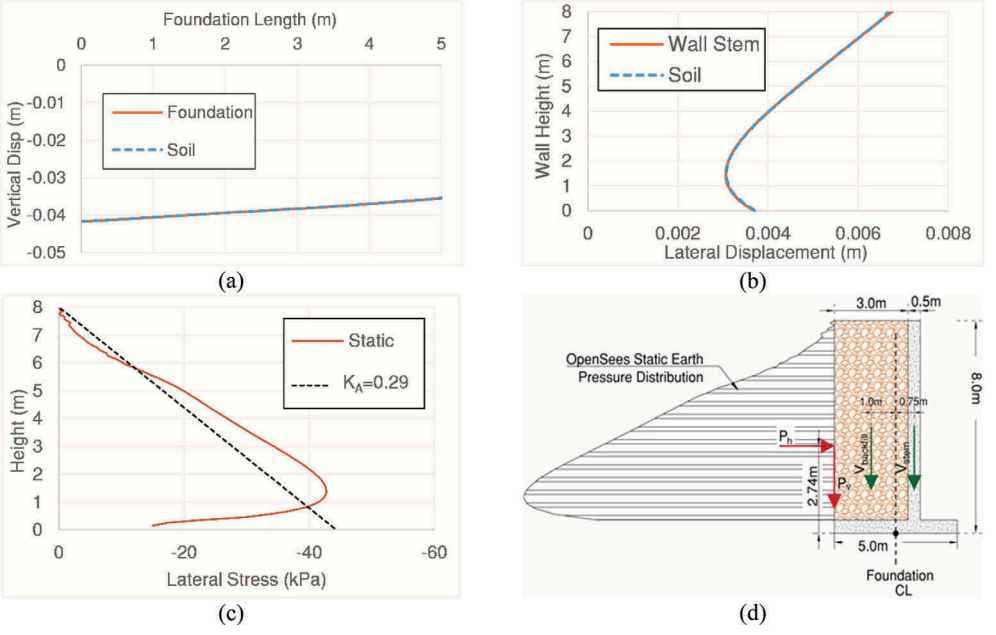

Figure 4. Static analysis a) foundation settlement, b) wall stem horizontal displacement, c) gravity earth pressure distribution and, d) free body diagram of existing forces on the wall during gravity analysis

Further observation of the free body diagram of the wall and backfill lab in Figure 4d can reveal the reason of foundation rotation towards the backfill. The forces participating in the rotation of the foundation are stem weight (V_{stem}), backfill weight ($V_{backfill}$), the horizontal component of static earth thrust (P_h) and, the vertical component of static earth thrust (P_v). Calculating the sum moment of these forces around the foundation centre line gives us a counterclockwise moment.

3.2 *Dynamic phase*

Pender (2018) found for a similar type of retaining wall the horizontal acceleration to trigger the failure was 0.27g. Therefore, the excitations in this study are selected so that the response of centroid of backfill block (centroid of the soil block in Figure 4d) would be more than 0.27g. The model is subjected to two Ricker wavelet inputs with a frequency of 1.0Hz and maximum accelerations of 0.2g and 0.4g.

Four time steps for each input has been chosen to find the largest total (dynamic plus static) lateral earth pressure distribution. As shown in Figure 5a and b, three time steps at which the acceleration response of the backfill block centroid reached its major peaks and a time step at which the longest length of the foundation has been lifted. The maximum response accelerations of the centroid for 0.2g and 0.4g are approximately 0.4g and 0.6g respectively. The longest detached lengths of the foundation for 0.2g and 0.4g are 30 and 90cm respectively.

Figure 5c and d are illustrating the largest total earth pressure distribution occurred at the time step of the second largest peak of the centroid. On the other hand, the earth pressures at the time step of the maximum response accelerations in both input cases are even smaller than the static earth pressure.

For the 0.2g input case, the maximum equivalent earth thrust is 427 kN located at 2.87m of the base of the wall. The M-O method is showing for this case K_{AE}=0.62 thus the equivalent force is 375 kN situated at 2.67m from the base of the wall. Therefore, the rotational moment of the dynamic analysis is 22 percent higher than the M-O method for the 0.2g input case. Furthermore, for the 0.4g input, the earth thrusts from the dynamic analysis and M-O method are 537 and 618 kN located at 3.0 and 2.67m from the base of the wall respectively.

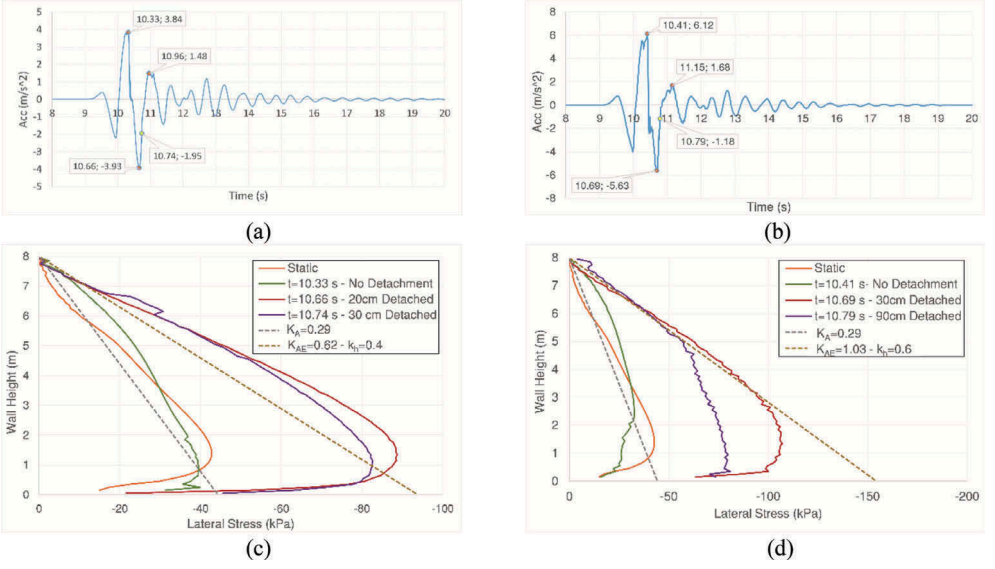

Figure 5. Response acceleration time history of the backfill centroid for the inputs a) 0.2g and, b) 0.4g. Earth pressure distribution of the inputs c) 0.2g and, d) 0.4g.

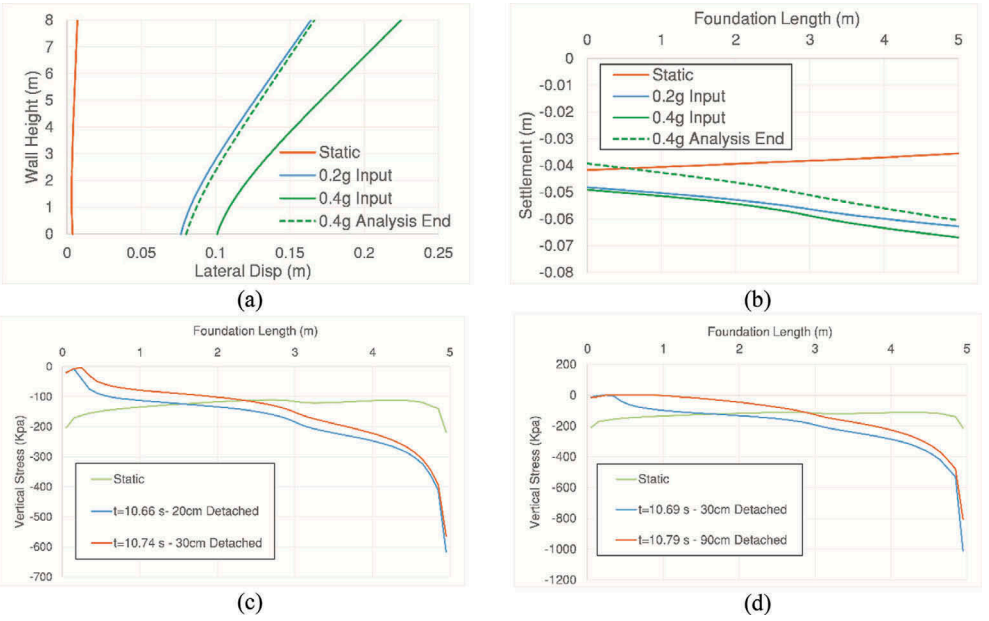

Figure 6. a) wall stem horizontal displacement and, b) foundation settlement. Existing bearing stresses of the foundation for the inputs c) 0.2g and, d) 0.4g.

Figure 6a and b show the horizontal and vertical displacements of the wall stem and the foundation respectively. The curves "0.2g Input" and "0.4 Input" represent displacements at the time step where the earth pressure is at its peak and "0.4g Analysis End" shows the permanent displacements at the end of the dynamic analysis. As can be seen, for the 0.2g input the foundation move 8cm against the backfill while the relative displacement of the wall top is 8cm. For 0.4 case, the maximum horizontal movement of the foundation is 10cm, and the relative displacement of the wall top is 12cm. The residual displacement of the wall stem is close to the maximum displacements of the 0.2g case. Also, the permanent effect of wavelet input can be observed by comparing permanent settlement of the foundation for the 0.4g case with the static case in Figure 6b. As is shown, although the forces in the model are equal in the static and by the end of dynamic analyses, the rotations of the foundations are completely different.

Figure 6c and d imply that the existing bearing stresses under the foundation are compliant with the settlements of Figure 6b. Existing bearing stresses zero or close to zero are showing uplift of the foundation in Figure 6c and d.

4 CONCLUSIONS

The static and dynamic responses of a gravity retaining wall have been investigated for different Ricker wavelet excitations. A series of site response analysis on a 1D soil column have been conducted to choose the suitable Ricker wavelets for the main retaining wall model. The main retaining wall model has a dry medium and dense cohesionless sand as the backfill and underlying soil respectively. The constitutive model used to represent the soil is that of Manzari and Dafalias. The conclusions drawn from this study are:

- The site response analyses have implied linear soil might not be a good representative of the soil and can result in overestimation of the earth pressures. The ratio between the maximum acceleration of the response and the input for elastic soil can be more than twice that of the nonlinear cohesionless soil.
- Choosing a Ricker wavelet with a fundamental period of T=1s gives the most response of the backfill behind the wall.

- During the gravity analysis, tilting direction of the retaining wall depends on the geometry of the wall, density of the backfill block and friction angle of the backfill and the interface. The assumption that the wall would tilt away from the backfill might not be correct in all cases.
- Apart from the frequency, the maximum acceleration of the input has an effect on the response. While for 0.2g input the peak acceleration response doubled, for the 0.4g input, it increased by a factor 1.5. This is due to soil nonlinearity.
- There can be a delay between the occurrence of the peak acceleration response and the maximum earth thrust. The maximum earth thrust took place almost 0.7s after the input peak acceleration for 0.4g case.
- Comparing to the Mononobe-Okabe method, the earth thrust point of application for 0.2g and 0.4g input is not significantly different. Also, in agreement with Mikola et al. (2014), Chin et al. (2016), and Wood (2018) work, judging by the distribution shape, an upright triangle is a better representation for the earth pressure distribution.

ACKNOWLEDGMENT

This study is funded by the University of Canterbury Quake Centre (UCQC). All the analyses have been done through Mahuika platform of New Zealand e-Science Infrastructure (NeSI). The generous advice of Dr Christopher McGann, Dr Alborz Ghofrani and, Mr Yuri Wong is greatly appreciated.

REFERENCES

Al Atik, L. & Sitar, N. 2010. Seismic Earth Pressures on Cantilever Retaining Structures. Journal of Geotechnical and Geoenvironmental Engineering, 136, 1324-1333.

Antoniou, S., Pinho, R. & Bianchi, F. 2008. SeismoSignal. Version 3.2. 0.

Chin, C. Y., Kayser, C. & Pender, M. 2016. Seismic Earth Forces Against Embedded Retaining Walls: Insights from Numerical Modelling. Bulletin of the New Zealand Society for Earthquake Engineering, 49, 200-210.

Coll, A., Ribo, R., Pasenau, M., Escolano, E., Perez, J. S., Melendo, A., Monros, A. & Ga, R. J. 2016. GiD v.13 User Manual [Computer Software].

Dafalias, Y. F. & Manzari, M. T. 2004. Simple Plasticity Sand Model Accounting for Fabric Change Effects. Journal of Engineering Mechanics, 130, 622-634.

Drumm, E. C. & Desai, C. S. 1986. Determination of parameters for a model for the cyclic behaviour of interfaces. Earthquake Engineering & Structural Dynamics, 14, 1-18.

Fardis, N., Georgarakos, P., Gazetas, G. & Anastasopoulos, I. Sliding Isolation of Structures: Effect of Horizontal and Vertical Acceleration. Fib International Symposium on Concrete Structures in Seismic Regions, 2003 Athens, 6–8 May.

Joyner, W. B. & Chen, A. T. F. 1975. Calculation of nonlinear ground response in earthquakes. Bulletin of the Seismological Society of America, 65, 1315-1336.

Kolay, C., Prashant, A. & Jain, S. K. 2013. Nonlinear Dynamic Analysis and Seismic Coefficient for Abutments and Retaining Walls. Earthquake Spectra, 29, 427-451.

Lysmer, J. & Kuhlemeyer, R. L. 1969. Finite dynamic model for infinite media. Journal of the Engineering Mechanics Division, 95, 859-878.

Mcgann, C. R. & Arduino, P. 2015. Dynamic 2D Effective Stress Analysis of Slope (http://opensees.berkeley.edu/wiki/index.php/Dynamic_2D_Effective_Stress_Analysis_of_Slope). [Accessed 29 August 2017].

Mckenna, F., Mazzoni, S. & Fenves, G. 2013. Open System for Earthquake Engineering Simulation (OpenSees) Software Version 2.5.0 [Computer Software]. University of California, Berkeley, CA. Available from http://opensees.berkeley.edu.

Mikola, R. G., Candia, G. & Sitar, N. Seismic earth pressures on retaining structures and basement walls. Tenth US national conference on earthquake engineering, frontiers of earthquake engineering. Anchorage, Alaska, 2014.

Mononobe, N. & Matsuo, H. On the determination of earth pressures during earthquakes. World Engineering Congress, 1929 Tokyo, Japan.

Okabe, S. 1924. General theory on earth pressure and seismic stability of retaining wall and dam. J. of Japan Society of Civil Engineers, 10, 1277-1323.
Pender, M. J. 2018. Foundation design for gravity retaining walls under earthquake. Proceedings of the Institution of Civil Engineers - Geotechnical Engineering, https://doi.org/10.1680/jgeen.17.00233.
Seed, H. B. & Whitman, R. V. Design of Earth Retaining Structures for Dynamic Loads. ASCE Specialty Conference, Lateral Stresses in the Ground and Design of Earth Retaining Structures, 1970 Cornell Univ., Ithaca, New York. 103-147.
Sitar, N. & Al Atik, L. 2008. Dynamic centrifuge study of seismically induced lateral earth pressures on retaining structures. Geotechnical Earthquake Engineering and Soil Dynamics IV.
Sitar, N., Mikola, R. G. & Candia, G. 2012. Seismically induced lateral earth pressures on retaining structures and basement walls. Geotechnical Engineering State of the Art and Practice: Keynote Lectures from GeoCongress 2012.
Standards New Zealand Technical Committee 2004. Structural design actions (NZS 1170.5: 2004). Wellington, New Zealand.
Wood, J. H. 2018. Earthquake design of flexible soil-retaining structures. Proceedings of the Institution of Civil Engineers - Geotechnical Engineering, https://doi.org/10.1680/jgeen.17.00192.